Title
Directive emission from a single subwavelength aperture in a periodically corrugated silver film

ISBN
978-0-8194-6709-6

Authors
Capolino, Filippo
Qiang, Rui
Jackson, David R
et al.

Publication Date
2007-05-04

DOI
10.1117/12.725948

Directive Emission from a Single Subwavelength Aperture in a Periodically Corrugated Silver Film

Filippo Capolino*[ab], Rui Qiang[b], David R. Jackson[b], and Ji Chen[b]
[a]Department of Information Engineering, University of Siena, 53100 Siena, Italy;
[b]Dept. of Electrical and Computer Engineering, University of Houston, Houston, TX 77204, USA.

ABSTRACT

We present here an algorithm to evaluate the field in the near zone produced by a finite-size electromagnetic source in a periodic structure, referred to as the array scanning method (ASM) - FDTD method. Using a frequency-dependent silver permittivity model, obtained from measurement at optical and infrared frequencies, we implemented the corresponding modeling equations in the ASM-FDTD algorithm using the Z-transform technique. The developed algorithm is applied to the study of the enhanced radiation of a magnetic line source in a corrugated silver film, and the results indicate that the enhancement is due to the excitation of a leaky mode. We also show that other waves may be excited by the source depending on its location, and how this affects the radiation pattern.

Keywords: Surface plasmon, beaming, enhanced transmission, periodic structure, leaky mode.

1. INTRODUCTION

Highly directive beams at optical wavelengths arising from an illuminated single subwavelength slit or hole in a corrugated metal film such as silver have been observed recently, along with enhanced transmission properties [1]-[5]. It is known that this phenomenon is due to the excitation of a surface plasmon (SP) at the metal-air interface. Numerous investigations have analyzed the role of the geometry and frequency on the beam properties.

Here we model the slit by using an equivalent magnetic line-source current. Two possible locations for the source are analyzed. We first show a new algorithm referred to as array scanning method (ASM), whose preliminary results have been published in [6], which enables the evaluation of the field on an infinite periodic structure excited by a single source, such as a magnetic line source. The ASM algorithm requires the analysis of only a single periodic cell of the structure (even though the structure is excited by a single source). When combined with the FDTD method the new algorithm permits savings of both memory and solution time compared with the standard FDTD method (which must include many periodic cells in the stimulation domain in order to obtain an accurate solution). The FDTD method for periodic structures is here implemented with the "phase shift" boundary conditions in the time domain [7]-[11]. This is a new implementation of the FDTD method that permits the analysis of time-varying excitations in periodic structures illuminated by a plane wave with oblique incidence or by a periodic set of line sources phased to produce a beam at an oblique angle.

We also use a permittivity dispersive model used for silver based on measurements at optical and infrared frequencies [12], suitable for an FDTD implementation. The dispersive behavior is taken into account in the FDTD method by using the Z-transform technique [13].

In addition to the new algorithm for periodic structures made of dispersive materials, we also provide a simple and physical description of the enhanced directivity phenomena in terms of leaky modes. The slit excites two types of fields: a space wave (similar to the space wave radiated from a source in free space, but now with spatial harmonics present) and a SP mode. This is a general property of the field in periodic structures excited by a localized source and more details are given in [14].

Metamaterials II, edited by Vladimir Kuzmiak, Peter Markos, Tomasz Szoplik,
Proc. of SPIE Vol. 6581, 65810E, (2007) · 0277-786X/07/$18 · doi: 10.1117/12.725948

We show that the field at the silver-air interface is dominated by a leaky mode, which is a radiating mode guided by the structure. The leaky mode is the SP mode that becomes leaky (radiating) due to the presence of the periodic corrugations. Therefore, this structure is similar in principle to a leaky-wave antenna that is scanned to broadside. For these structures it is the n = -1 Floquet spatial harmonic of the guided mode (the one in the visible region) that is radiating. Because of this radiation, the surface plasmon is a leaky mode that has a complex wavenumber. We also show, as a preliminary example, the effect of the space wave in our sample geometry. Although the leaky mode will dominate the radiation pattern near the peak of the beam for a highly directive beam, the space wave may have a considerable influence on the beam shape for less directive situations.

To study these effects, it is necessary to perform comprehensive full-wave electromagnetic modeling. Conventional approaches for analyzing such structures via FDTD simulations often use several hundred periodic elements in the modeling. In this paper, the above-mentioned full-wave FDTD simulations combined with the array scanning method (ASM), is found to be much more efficient, since only the FDTD modeling of a single periodic cell is required.

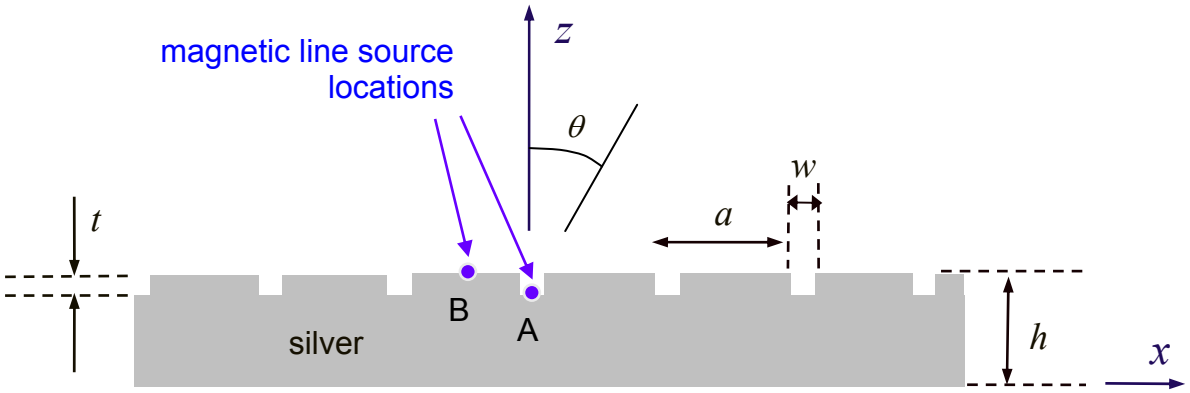

Fig. 1. Geometry of the silver film with corrugations, excited by an infinite magnetic line current at location A or B. Geometry parameters: $w = t = 40$ nm, $a = 650$ nm, $h = 350$ nm.

2. THE ASM-FDTD METHOD

2.1 ASM-FDTD Method for Near Field Calculation

In this paper, only the case of a transverse magnetic (TM_z) field is considered, corresponding to a structure that is invariant in the y direction, illuminated by an infinite magnetic line source. Consider, as an example, the structure in Fig. 1, where a is the period along x and $\mathbf{r}_0$ is the location of the magnetic line source that produces a magnetic field H_y , which is henceforth referred to simply as H. The observation point in an arbitrary periodic cell n (Fig. 1) is denoted by $\mathbf{r} + na\mathbf{1}_x$, where $\mathbf{r}$ is defined in the n = 0 periodic cell, and $\mathbf{1}_x$ is the unit vector along x. In the time domain the ASM representation of the total field at $\mathbf{r} + na\mathbf{1}_x$, produced by the single source in the periodic environment, is [6]

$$\hat{H}_{tot}(\mathbf{r},\mathbf{r}_0,t)=\frac{a}{2\pi}\int_{-\pi/a}^{\pi/a}\hat{H}_{tot}^{\infty}(\mathbf{r},\mathbf{r}_0,k_x,t)\,dk_x\,. \tag{1}$$

where the hat ^ tags time-domain (TD) quantities. The "∞" superscript denotes the field due to an infinite phased array of line sources, with phasing wavenumber k_x. In the TD the field quantities are complex [7]-[10] and a periodic boundary condition at the edges of the periodic cell are assumed, corresponding to the wavenumber k_x. For example, the magnetic field $\hat{H}_{tot}^{\infty}$ satisfies

$$\hat{H}_{tot}^{\infty}(\mathbf{r}+a\mathbf{1}_x,\mathbf{r}_0,k_x,t)=\hat{H}_{tot}^{\infty}(\mathbf{r},\mathbf{r}_0,k_x,t)\,e^{-jk_xa}\,. \tag{2}$$

Equation (2) makes it obvious that in this rather unusual TD application the TD field $\hat{H}_{tot}^{\infty}(\mathbf{r},\mathbf{r}_0,k_x,t)$ is represented as a complex function. To implement the periodic boundary condition (2) using the FDTD method, the phasing parameter k_x needs to be discretized within the fundamental Brillouin zone. In our implementation, an even number N_{kx} of spectral sampling points, uniformly distributed over the fundamental Brillouin zone, is used. Spectral FDTD simulations are carried out at every spectral sampling point k_x using the boundary condition described by (2) [10]. Since complex values described in (2) are used in the FDTD implementation, both electric and magnetic field values are complex. The spectral sampling points are located at

$$k_x=\xi_i=\pi a^{-1}\left[-1+(2i-1)/N_{kx}\right],\quad \text{with}\quad i=1,...,N_{kx}\,, \tag{3}$$

After the computed field $\hat{H}_{tot}^{\infty}(\mathbf{r},\mathbf{r}_0,\xi_i,t)$ is obtained at all the sample points, the time-domain field within any periodic cell, produced by the single line source at $\mathbf{r}_0$, can be evaluated by adding all the computed fields. For example, using the simple rectangle rule of integration, we have

$$\hat{H}_{tot}(\mathbf{r}+na\mathbf{1}_x,\mathbf{r}_0,t)=\frac{1}{N_{kx}}\sum_{i=1}^{N_{kx}}\hat{H}_{tot}^{\infty}(\mathbf{r},\mathbf{r}_0,\xi_i,t)\,e^{-jna\xi_i}\,. \tag{4}$$

It should be noted that other quadrature schemes can be used (e.g., Gaussian quadrature) but they do not necessarily increase the numerical accuracy, since the rectangle rule of integration is usually very efficiency for smooth periodic functions. It should also be pointed out that if a real-valued excitation is used, the final value of (1) is also real-valued. The detailed implementation of the spectral FDTD is as in [7]-[11].

2.2 Temporal Dispersion in the FDTD Method for the Silver Material

To implement the frequency-dependent dielectric behavior of silver at IR and optical wavelengths, we have used a model based on measurement data. This model is described by a Lorentz-Drude formula that approximates the complex permittivity of the silver film in the IR regime as [12]

$$\varepsilon_r(\omega)=\varepsilon_r^f(\omega)+\varepsilon_r^b(\omega)=\left(1-\frac{\Omega_p^2}{\omega(\omega-j\Gamma_0)}\right)+\left(\sum_{i=1}^{k}\frac{f_i\omega_p^2}{(\omega_i^2-\omega^2)+j\omega\Gamma_i}\right) \tag{5}$$

where $\varepsilon_r^f(\omega)$ and $\varepsilon_r^b(\omega)$ correspond to inter-band Drude and Lorentz models, respectively. In the equation above, ω_p is the plasma frequency, k is the number of oscillators with frequency ω_i, strength f_i, and lifetime $1/\Gamma_i$, while $\Omega_p = \sqrt{f_0}\omega_p$. A detailed definition of these parameters and the values for these parameters for different films can be found in [12]. In Fig. 2 we show the frequency dependence of the real and imaginary parts of the permittivity produced by this model as well as by a lossless Drude model.

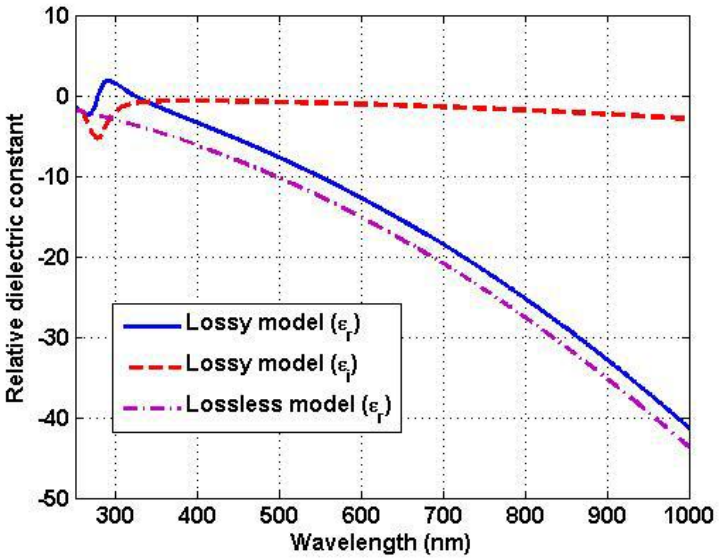

Fig. 2. Real (blue) and imaginary (red) part of the relative permittivity $\varepsilon = \varepsilon_r + j\varepsilon_i$ for silver, calculated by the Lorentz-Drude model as given by (5), as a function of wavelength. Also shown in the result for a lossless silver film, given by the Drude model. The model is from [12].

The major steps to incorporate the Lorentz-Drude model in the FDTD method can be described as follows.

1. Relate the frequency-domain electric flux density to the electric field by $D(\omega) = \varepsilon_0 \varepsilon_r(\omega) E(\omega)$, where $\varepsilon_r(\omega)$ is given in (5).

2. Transform (5) via the Z transform to obtain [13]

$$D(z) = \varepsilon_0 E(z) + z^{-1} S_1(z) + z^{-1} S_2(z), \tag{6}$$

where $z^{-1}S_1$ is the Z transformation for the Drude model and $z^{-1}S_2$ is for the Lorentz model, given by

$$S_1(z) = \varepsilon_0 \frac{\Omega_p^2 \Delta t}{\Gamma_0}\left[\frac{\left(1-e^{-\Gamma_0 \Delta t}\right)}{1-\left(1+e^{-\Gamma_0 \Delta t}\right)z^{-1}+1-e^{-\Gamma_0 \Delta t}z^{-2}}\right]E(z)$$
$$S_2(z) = \varepsilon_0 \sum_{i=1}^{k} \frac{f_i \omega_p^2}{\beta_i} \frac{e^{-\alpha_i \Delta t}\sin\left(\beta_i \Delta t\right)\Delta t}{1-2e^{-\alpha_i \Delta t}\cos\left(\beta_i \Delta t\right)z^{-1}+e^{-2\alpha_i \Delta t}z^{-2}}E(z). \quad (7)$$

Based on equations above, $E(z)$ can be obtained by

$$E(z) = \frac{1}{\varepsilon_0}\left[D(z) - z^{-1}S_1(z) - z^{-1}S_2(z)\right]. \quad (8)$$

3. Replacing $E(z)$ with E^{n+1}, $z^{-1}E(z)$ with E^n to obtain the electric field. This leads to

$$E^{n+1} = \frac{1}{\varepsilon_0}\left[D^{n+1} - \left(S_1^n + S_2^n\right)\right]$$
$$S_1^{n+1} = \left(1+e^{-\Gamma_0 \Delta t}\right)S_1^n - e^{-\Gamma_0 \Delta t}S_1^{n-1} + \varepsilon_0 \frac{\Omega_p^2 \Delta t}{\Gamma_0}\left(1-e^{-\Gamma_0 \Delta t}\right)E^{n+1} \quad (9)$$
$$S_2^{n+1} = \sum_{i=1}^{k}\left[2e^{-\alpha_i \Delta t}\cos\left(\beta_i \Delta t\right)S_2^n - e^{-2\alpha_i \Delta t}S_2^{n-1} + \varepsilon_0 \frac{f_i \omega_p^2}{\beta_i}e^{-\alpha_i \Delta t}\sin\left(\beta_i \Delta t\right)\Delta t E^{n+1}\right].$$

The model for a lossless silver film is obtained by simply modifying the parameters in (5). For the wavelength of our interest here (around 700 nm), the multi-term Lorentz model (the second term in (5)) can then be removed in (5) since it does not have a significant effect on the real part of permittivity. To enforce the imaginary part equal to zero at a particular wavelength, we simply set the parameter Γ_0 in the Drude model either close to zero or to a very small number. Consequently, the permittivity of a lossless silver film can be represented in the simple Drude model as

$$\varepsilon_r(\omega) = 1 - \frac{\Omega_p^2}{\omega^2} \quad (10)$$

The permittivity described by (10) is shown by the purple curve in Fig. 2. It is clear that the model given in (10) is a good approximation to the real part of lossy model in (5). Applying the similar principle as in (9), the field updating equations used in FDTD method then become in the lossless case as

$$E^{n+1} = \frac{1}{\varepsilon_0}\left[D^{n+1} - S_1^n\right] \quad (11)$$

where

$$S_1^{n+1} = 2S_1^n - S_1^{n-1} + \varepsilon_0 \Omega_p^2 \Delta t^2 E^{n+1}. \quad (12)$$

3. FAR-FIELD RADIATION PATTERN FOR THE PLASMONIC CORRUGATED SILVER FILM

Here we show the radiation pattern produced by a magnetic line source that is placed at location A or B shown in Fig. 1, on the surface of the corrugated silver film. The geometry parameters are those in the caption of Fig. 1. Locations A and B are in the middle of a groove and on the top surface of the film, respectively. In the past the enhanced directivity effect has been demonstrated for a similar structure with a slit connecting the bottom and the top surfaces, with the bottom face illuminated by a beam. The magnetic line source here is intended to model the equivalent magnetic current that is placed on the slit aperture after the equivalence principle is applied.

The far filed pattern due to the magnetic current line source excitation at point A or B can be obtained using the reciprocity theorem. The theorem states that the far field pattern can be evaluated by sampling the magnetic field value at positions A or B when a plane wave is launched towards the structure from different angles of incidence. For this particular case, this theorem can be easily implemented with the use of the periodic boundary technique described above, and the simulation is performed within only one periodic cell. The far-field patterns are plotted in Fig. 3. The maximum always occurs at broadside (i.e., at $\theta = 0°$) and an extremely narrow beam width is also observed. The "optimum" wavelength is the one that produces the maximum radiated field at broadside. Its value slightly depends on the source location, and the two optimum wavelengths related to the source location at A or B are shown in Table 1.

This enhanced directivity, previously noted in various publications [1]-[5] is here explained by noticing that there is a leaky mode (a surface plasmon with complex propagation wavenumber) traveling along the air-silver interface. The magnetic source, either at point A or B, excites both the leaky-mode as well as a space-wave contribution. The strengths of these two very different wave fields depend on the source location, and therefore the total-field radiation patterns produced by an excitation at A or B are slightly different. In Fig. 3, when the source is at point A, the null at $\theta = \pm 3°$ is due to the cancellation effect of these two types of contributions (the leaky mode and the space wave). We have experienced other cases where the space- wave field has a more pronounced effect. In general, the space wave has a stronger influence when the structure has more loss, so that the leaky mode is attenuated more rapidly.

The different, although small, effect of the space-wave contribution for excitation at point A or B explains why the optimized wavelengths for points A and B are slightly different.

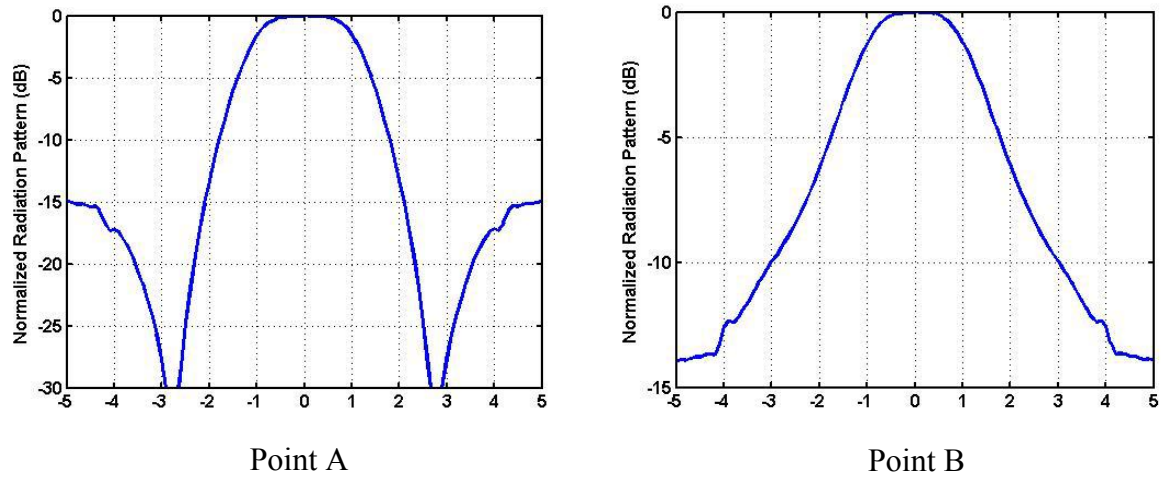

Fig. 3. Far-field radiation patterns for excitation at points A and B for the lossy case, $t = 40$ nm.

	Location A	Location B
Optimized operating wavelength	$\lambda_A = 698.9$ nm	$\lambda_B = 696.8$ nm

Table 1. Optimized wavelengths for excitation at point A or B. The two optimized wavelengths are slightly different.

4. INTERFACE FIELD FOR THE PLASMONIC CORRUGATED SILVER FILM

Since the far-field radiation patterns are closely related to the field at the interface between the air and the silver film, in this section we use the developed ASM-FDTD method to evaluate and analyze the interface field along the x direction (Fig. 1). The depth of the grove is still 40 nm, and a lossy silver model is used. In the simulation, the FDTD mesh size in both the x and z directions is set to be 10 nm. A sinusoidal oscillating magnetic current line source with an operating wavelength of $\lambda_A = 698.9$ nm resides at point A. The conventional FDTD method is also applied to validate the accuracy of the ASM-FDTD method. However, in the simulation performed by the conventional FDTD method, in order to emulate the infinite periodicity in the x direction, at least 600 periodic until-cells are modeled in the computation domain. Therefore the structure is large enough to attenuate the leaky plasmon mode before it reaches the edges of the structure. The ASM-FDTD technique provides a more efficient way to simulate the infinite structure with a dramatically reduced computer memory requirement. The magnitude of the magnetic field H_y (x) at the interface, sampled at each unit cell, is calculated by both the FDTD and ASM-FDTD methods, and the results are plotted in Fig. 4. We see that the solutions obtained by two methods show no noticeable difference up to 50 unit cells away from the source location. Though the silver film is lossy, a stronger exponential decay along the x direction is observed compared to that which would be expected due to loss alone, and this demonstrates that a leaky mode is excited. Since the radiated field (with a narrow beam) is produced by the radiation of the equivalent current on the air-film interface, the far-field pattern is well predicted by the leaky mode that is excited by the source.

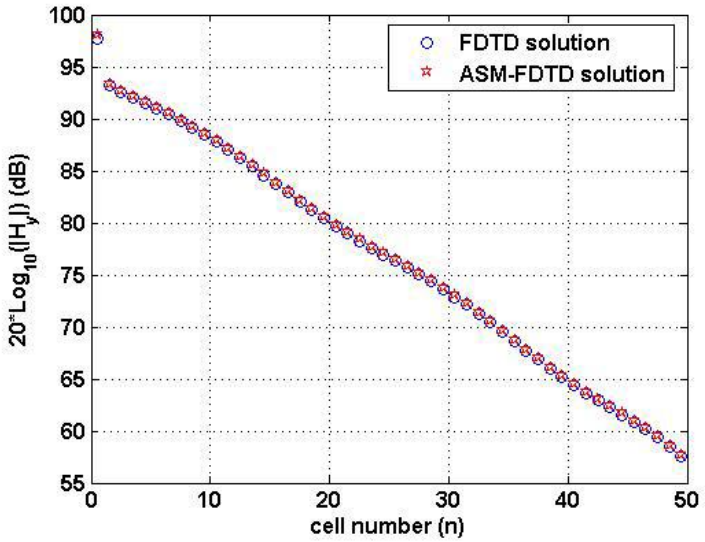

Fig. 4. Interface field calculated along the interface between air and the silver film, when the structure is excited at point A. A lossy silver film is considered, with $t = 40$ nm.

REFERENCES

1. T. Thio, K. M. Pellerin, R. A. Linke, H. J. Lezec, and T. W. Ebbesen, "Enhanced light transmission through a single subwavelength aperture," *Opt. Lett.*, vol. 26, pp. 1972–1974, Dec. 2001.
2. T. Thio, H. J. Lezec, T. W. Ebbesen, K. M. Pellerin, G. D. Lewin, A. Nahata, and R. A. Linke "Giant optical transmission of sub-wavelength apertures: physics and applications," *Nanotechnology*, vol. 13, pp. 429–432, June 2002.
3. H. J. Lezec, A. Degiron, E. Devaux, R. A. Linke, L. Martin-Moreno, F. J. Garcia-Vidal, and T. W. Ebbesen, "Beaming of Light from a Subwavelength Aperture," Science, vol. 297, pp. 820-822, Aug. 2, 2002.
4. L. Martin-Moreno, F. J. Garcia-Vidal, H. J. Lezec, A. Degiron, and T. W. Ebbesen, "Theory of highly directive emission from a single subwavelength aperture surrounded by surface corrugations," *Phys. Rev. Lett*., vol. 90, pp. 167401-1 – 167401-4, Apr. 2003.
5. F. J. Garcı´a-Vidal, H. J. Lezec, T.W. Ebbesen, and L. Martı´n-Moreno, "Multiple Paths to Enhance Optical Transmission through a Single Subwavelength Slit", *Physical Review Letters*, Vol. 90, No. 21, May 30, 2003
6. R. Qiang, J. Chen, F. Capolino, D. R. Jackson, and D. R. Wilton, "Array Scanning Method-FDTD for Emission of Finite Electromagnetic Sources in Periodic Artificial Materials," *IEEE Microwave on Wireless Components Letters,* Vol. April, 2007.
7. A. C. Cangellaris, M. Gribbons, and G. Sohos, "A hybrid spectral/FDTD method for the electromagnetic analysis of guided waves in periodic structures," *IEEE Microwave Guided Wave Lett.*, Vol. 3, pp. 375-377, March 1993.
8. A. Aminian and Y. Rahmat-Samii, "bandwidth determination for soft and hard ground planes by spectral FDTD: a unified approach in visible and surface waver regions," *IEEE Trans. Antennas and Propagat.*, vol. 53, no. 6, pp. 18-28, Jan. 2005.
9. A. Aminian and Y. Rahmat-Samii, "Spectral FDTD: a novel technique for the analysis of oblique incident plane wave on periodic structures," *IEEE Trans. Antennas and Propagat.*, vol. 54, no. 6, pp. 1818-1825, June 2006.
10. Fan Yang, Ji Chen, Rui Qiang, and Atef Elsherbeni, "FDTD analysis of periodic structures at arbitrary incidence angles: a simple and efficient implementation of the periodic boundary conditions", *IEEE Antennas and Propagation Society Intenl Symp.,* pp. 2715-2718, June 2006.
11. T. Kokkinos, C. D. Sarris, and G. V. Eleftheriades, "Periodic FDTD analysis of leaky-wave structures and applications to the analysis of negative-refractive-index leaky-wave antennas", *IEEE Trans. Microwave Theory and Techniques*, vol. 54, no. 4, pp.1619-1630, June 2006.
12. Rakic A. D., Djurisic A. B., Elazar J. M., and Majewski M. L., "Optical properties of metallic films for vertical-cavity optoelectronic devices", Applied Optics, August 1998, Vol. 37 No. 22, pp. 5271–5283.
13. Sullivan D. M., "Frequency-dependent FDTD methods using Z transforms', *IEEE Trans. Antenna and Propagat.*, vol. AP-40, Oct. 1992, pp.1223-1230.
14. F. Capolino, D. R. Jackson, and D. R. Wilton, "Fundamental Properties of the Field at the Interface Between Air and a Periodic Artificial Material Excited by a Line Source," *IEEE Trans. Antennas Propagat.*, Vol. 53, pp. 91–99, Jan. 2005.